

## Walking in the 3-dimensional large $N$ scalar model

---

Sinya Aoki,<sup>a,b</sup> Janos Balog,<sup>c</sup> Peter Weisz<sup>d</sup>

<sup>a</sup> *Yukawa Institute for Theoretical Physics, Kyoto University,  
Kitashirakawa Oiwakechou, Sakyo-ku, Kyoto 606-8502, Japan*

<sup>b</sup> *Center for Computational Sciences, University of Tsukuba 305-8577, Japan*

<sup>c</sup> *Institute for Particle and Nuclear Physics, Wigner Research Centre for Physics,  
MTA Lendület Holographic QFT Group, 1525 Budapest 114, P.O.B. 49, Hungary*

<sup>d</sup> *Max-Planck-Institut für Physik, 80805 Munich, Germany*

*E-mail:* [saoki@yukawa.kyoto-u.ac.jp](mailto:saoki@yukawa.kyoto-u.ac.jp), [balog.janos@wigner.mta.hu](mailto:balog.janos@wigner.mta.hu),  
[pew@mpp.mpg.de](mailto:pew@mpp.mpg.de)

**ABSTRACT:** The solvability of the three-dimensional  $O(N)$  scalar field theory in the large  $N$  limit makes it an ideal toy model exhibiting "walking" behavior, expected in some  $SU(N)$  gauge theories with a large number of fermion flavors. We study the model using lattice regularization and show that when the ratio of the particle mass to an effective 4-point coupling (with dimension mass) is small, the beta function associated to the running 4-point coupling is "walking". We also study lattice artifacts and finite size effects, and find that while the former can be sizable at realistic correlation length, the latter are under control already at lattice sizes a few ( $\sim 3$ ) correlation lengths. We show the robustness of the walking phenomenon by showing that it can also be observed by studying physical observables such as the scattering phase shifts and the mass gap in finite volume.

**KEYWORDS:** 3-dimensional  $O(N)$  scalar field theory, large  $N$  limit, walking coupling, beta function, scattering phase shift

---

## Contents

<b>1</b>	<b>Introduction</b>	<b>1</b>
<b>2</b>	<b>Large <math>N</math> expansion of the lattice model</b>	<b>3</b>
2.1	Large $N$ saddle point expansion	4
2.2	VEV and Correlation functions	6
<b>3</b>	<b>Renormalization and continuum limits</b>	<b>7</b>
3.1	Continuum limits in the symmetric phase	8
3.2	Continuum limits in the broken phase	9
3.3	6-pt vertex function for $\pi$ fields	11
<b>4</b>	<b>Running four-point coupling</b>	<b>12</b>
4.1	Beta function	12
4.2	Lattice artifact and finite size corrections to the "walking" behavior of the beta function	13
<b>5</b>	<b>Scattering phase shifts</b>	<b>15</b>
5.1	Scattering amplitude	15
5.2	Unitarity and scattering phase shift	17
<b>6</b>	<b>Summary</b>	<b>18</b>
<b>A</b>	<b>Resonance parameters on the lattice</b>	<b>19</b>
<b>B</b>	<b>Finite-volume mass gap and running coupling</b>	<b>21</b>
B.1	Continuum limit(s)	22
B.2	Finite volume coupling	24

---

## 1 Introduction

The Standard Model (SM) is a truly remarkable effective theory, presently in agreement with all available electro-weak data (apart from a few tensions). However, in search of a more fundamental theory, it was proposed[1, 2] that a higher gauge theory, called technicolor (TC) (for a detailed review see [3]), could dynamically explain the electro-weak scale and the origin of masses of the gauge bosons.

The original TC models, however, had the difficulty that they could not give quark masses, and models proposed to overcome this, so-called extended TC (ETC) models [4, 5], have a tension between a suppression of effects caused by flavor-changing neutral currents and a large top quark mass. In addition, precise electroweak measurements give strong

constraints on the dynamics of TC models[6]. In order to overcome these difficulties, a class of asymptotically free so-called walking TC models, for which the characteristic dynamics changed very slowly in the low energy regime, was proposed[7–9]. This could occur if typical running couplings came close to conformal fixed points where the associated beta-functions became zero [10].

The walking phenomena in asymptotically free theories is a non-perturbative phenomenon and requires corresponding investigations such as numerical simulations of the lattice regularized theory. This program has been actively and systematically pursued recently [11] given the improvement of lattice technology to simulate dynamical fermions and with the motivation of finding an alternative to SUSY to describe physics beyond the SM. The most popular models in 4-dimensions studied so far are  $SU(N)$  gauge theories with a large number  $N_f$  of fermion flavors, or with fermions in higher representations. See recent reviews[12–19] for references to these activities. For gauge group  $SU(N)$  it is probable that walking sets in when  $N_f$  exceeds a certain value (still less than  $11N/2$  to maintain asymptotic freedom). Although there are reports that  $SU(3)$  gauge theory with  $N_f = 8$  show walking behavior [20], there is still some debate [21]. Unambiguous identification of walking phenomena is in these models extremely difficult and CPU intensive. This is not only due to the problem of efficiently simulating dynamical fermions, but also to the need to control systematic errors arising from finite ultra-violet cutoff (finite lattice spacings) and from finite volume effects [22, 23].

It is thus advantageous to have simple toy models at hand which show walking and where the systematic errors mentioned above can be investigated in detail. There are as yet not many toy models where walking phenomena have been studied. One recent example suggested by Negradi [24] and studied numerically by de Forcrand, Pepe and Wiese [25] is the non-linear  $O(3)$  model in two dimensions with a  $\theta$  term. In this model it was established that walking appears when the continuous parameter  $\theta$  is close to the value  $\pi$ .

In this paper we investigate properties of another simple model, the  $N$ -component scalar field theory in three dimensions in the large  $N$  limit. This model exhibits walking phenomena when a continuous parameter  $\alpha$ , the ratio of renormalized mass to an effective 4-point coupling (with dimension mass), is very small. Other aspects of this model have been frequently studied in the literature (see the review [26]). In this toy model many features can be studied analytically, for example the systematic sources of error in lattice simulations mentioned above.

The material presented in this paper is as follows. In sect.2 we define the model with a particular lattice regularization and discuss its large  $N$  approximation. In the simplest scenario the lattice model has two phases, one where the  $O(N)$  symmetry is retained and one where this symmetry is broken spontaneously. Section 3 discusses renormalization and various continuum limits which can be obtained by approaching the critical surface in various ways.

In section 4 we introduce a dimensionless running coupling defined naturally through the connected 4-point function in the symmetric phase and discuss its behavior in the various continuum limits. One case, which we call IIA, exhibits walking for small values of  $\alpha$ , and in a typical case we investigate the lattice artifacts. Section 5 discusses the

scattering phase shift in the various continuum limits, as an on-shell dynamical quantity which also shows walking for case IIA.

We end our presentation with a summary of our results. In addition there are two appendices. Appendix A discusses the parameters of the resonance present in the broken phase of the lattice regulated theory. In Appendix B we introduce a coupling running with the volume defined in terms of the mass gap in a finite volume with periodic boundary conditions. This coupling also exhibits walking in case IIA.

## 2 Large $N$ expansion of the lattice model

In this paper, we consider an  $N$  component scalar model in 3 dimensions, defined by the action

$$S = \int d^3x \left[ \frac{1}{2} \partial^\mu \phi(x) \cdot \partial_\mu \phi(x) + NV_{\text{cont}} \left( \frac{\phi^2(x)}{N} \right) \right], \quad (2.1)$$

where  $\phi^i(x)$  is an  $N$  component scalar field with  $i = 1, 2, \dots, N$ ,  $(\cdot)$  indicates an inner product of  $N$  component vectors such that  $\phi^2(x) \equiv \phi(x) \cdot \phi(x) = \sum_{i=1}^N \phi^i(x) \phi^i(x)$ , and  $V_{\text{cont}}$  is a potential term, which takes the form  $V_{\text{cont}}(s) = \frac{m_0^2}{2}s + \frac{g_4}{4!}s^2 + \frac{g_6}{6!}s^3$ , where  $m_0$  is the bare scalar mass,  $g_k$  is the bare coupling constant of the  $\phi^k$  interaction, whose canonical dimension is  $3 - k/2$ .

We put the above model on a 3 dimensional Euclidean lattice with periodic boundary conditions in all directions. Let us define the partition function with a source as

$$Z(J) = \int [\mathcal{D}\Phi] \exp \left\{ \sum_{\mathbf{n}} \left[ \sum_{\mu=0}^2 \Phi_{\mathbf{n}} \cdot \Phi_{\mathbf{n}+\hat{\mu}} - NU \left( \frac{1}{N} \Phi_{\mathbf{n}}^2 \right) + J_{\mathbf{n}} \cdot \Phi_{\mathbf{n}} \right] \right\}, \quad (2.2)$$

where  $\mathbf{n} = (n_0, n_1, n_2)$  with  $n_i \in \mathbf{Z}$ ,  $\hat{\mu}$  is the unit vector in the  $\mu$ -th direction, and  $[\mathcal{D}\Phi] = \prod_{\mathbf{n}, i} d\Phi_{\mathbf{n}}^i$  is the measure. The periodic boundary condition is implemented by

$$\Phi_{\mathbf{n}+L_0\hat{0}}^i = \Phi_{\mathbf{n}+L_1\hat{1}}^i = \Phi_{\mathbf{n}+L_2\hat{2}}^i = \Phi_{\mathbf{n}}^i, \quad (2.3)$$

where  $\mathbf{L} = (L_0, L_1, L_2)$  are large but finite integers. We can obtain correlation functions of  $\Phi$ 's from  $Z(J)$ , by taking its derivative with respect to  $J$ 's and then setting  $J_{\mathbf{n}}^i \rightarrow J_0^i \equiv \sqrt{N}H\delta^{iN}$ , where the constant external field  $H$  coupled only to  $N$ -th component of  $\Phi$  is introduced to handle a possible spontaneous breaking of  $O(N)$  symmetry.

A potential term on the lattice takes the form

$$U(S) = \frac{R}{2}S + \frac{U}{4!}S^2 + \frac{G}{6!}S^3 + \sum_{k \geq 4} G_k S^k, \quad (2.4)$$

where dimensionless field  $\Phi_{\mathbf{n}}$  and parameters  $R, U, G$  are related to the continuum ones via the lattice spacing  $a$  as

$$\Phi_{\mathbf{n}} = \sqrt{a}\phi(x = \mathbf{n}a), \quad R = m_0^2 a^2 + 6, \quad U = g_4 a, \quad G = g_6, \quad (2.5)$$

while  $G_{k \geq 4}$  on the lattice does not have an counterpart in the formal continuum theory (2.1). Of course, these relations are classical and thus are modified after renormalization. An existence of the lower bound of the potential  $U(S)$  requires that non-zero coefficient of the largest power of  $S$  must be positive. Near the continuum limit this requires that  $G \geq 0$ , and if  $G = 0$ , then  $U \geq 0$ . In this paper, for distinction between dimensionless and dimensional quantities, we use capital letters for dimensionless quantities as much as possible.

## 2.1 Large $N$ saddle point expansion

Preparing the large  $N$  expansion, we insert into the path integral

$$1 \equiv \int [\mathcal{D}\Omega] \prod_{\mathbf{n}} \delta \left( \Omega_{\mathbf{n}} - \frac{1}{N} \Phi_{\mathbf{n}}^2 \right) = \mathcal{N}_1 \int [\mathcal{D}\Lambda] [\mathcal{D}\Omega] \exp \left\{ -N \sum_{\mathbf{n}} i\Lambda_{\mathbf{n}} \left( \frac{1}{N} \Phi_{\mathbf{n}}^2 - \Omega_{\mathbf{n}} \right) \right\}, \quad (2.6)$$

where  $\mathcal{N}_1 = \left( \frac{N}{2\pi} \right)^V$  with  $V = L_0 L_1 L_2$ , so that  $\Phi$ -integral becomes Gaussian and can be performed. We then obtain

$$Z(J) = \mathcal{N}_2 \int [\mathcal{D}\Lambda] [\mathcal{D}\Omega] \exp[-N S_{\text{eff}}(\Lambda, \Omega, J)], \quad \mathcal{N}_2 = \mathcal{N}_1 (2\pi)^{NV/2} \quad (2.7)$$

where the effective action is given by

$$S_{\text{eff}}(\Lambda, \Omega, J) = \sum_{\mathbf{n}} [U(\Omega_{\mathbf{n}}) - i\Lambda_{\mathbf{n}} \Omega_{\mathbf{n}}] - \frac{1}{2N} \sum_{nm,i} J_{\mathbf{n}}^i (D^{-1}[\Lambda])_{nm} J_{\mathbf{m}}^i + \frac{1}{2} \text{Tr} \ln D[\Lambda], \quad (2.8)$$

and the matrix  $D[\Lambda_{\mathbf{n}}]$  here acts on an arbitrary vector  $F$  as

$$(D[\Lambda]F)_{\mathbf{n}} = 2(i\Lambda_{\mathbf{n}} - 3)F_{\mathbf{n}} - (\nabla^2 F)_{\mathbf{n}}, \quad (\nabla^2 F)_{\mathbf{n}} \equiv \sum_{\mu} (F_{\mathbf{n}+\hat{\mu}} + F_{\mathbf{n}-\hat{\mu}} - 2F_{\mathbf{n}}). \quad (2.9)$$

The large  $N$  limit corresponds to the saddle point, determined by the saddle point equations,

$$\frac{\partial S_{\text{eff}}(\Lambda, \Omega, J_0)}{\partial \Lambda_{\mathbf{n}}} = -\Omega_{\mathbf{n}} + (D^{-1}[\Lambda])_{nn} + H^2 \left( \sum_{\mathbf{m}} (D^{-1}[\Lambda])_{m\mathbf{n}} \right)^2 = 0, \quad (2.10)$$

$$\frac{\partial S_{\text{eff}}(\Lambda, \Omega, J_0)}{\partial \Omega_{\mathbf{n}}} = U'(\Omega_{\mathbf{n}}) - i\Lambda_{\mathbf{n}} = 0. \quad (2.11)$$

To obtain a solution to the second equation, we have to take  $i\Lambda_{\mathbf{n}}$  real at the saddle point. Assuming a translation invariant solution, we thus take

$$i\Lambda_{\mathbf{n}} = i\Lambda_0 \equiv 3 + \frac{M^2}{2} = \text{const.} \quad (M \geq 0), \quad \Omega_{\mathbf{n}} = \Omega_0 = \text{const.}, \quad (2.12)$$

with which eqs. (2.10) and (2.11) become

$$\frac{H^2}{M^4} + I(M) = \Omega_0, \quad (2.13)$$

$$3 + \frac{M^2}{2} = U'(\Omega_0), \quad (2.14)$$

where

$$I(M) = \frac{1}{V} \sum_{\mathbf{K}} \frac{1}{\hat{\mathbf{K}}^2 + M^2}, \quad (2.15)$$

with

$$\hat{\mathbf{K}}^2 = \sum_{\nu} \hat{K}_{\nu}^2, \quad \hat{K}_{\nu} = 2 \sin \frac{K_{\nu}}{2}, \quad \mathbf{K} = 2\pi \left( \frac{l_0}{L_0}, \frac{l_1}{L_1}, \frac{l_2}{L_2} \right), \quad (2.16)$$

and  $l_{\mu}$ 's are integers which satisfy  $0 \leq l_{\mu} \leq L_{\mu} - 1$ . Later we will solve these equations explicitly in detail.

As is well known [26–29], it is possible to systematically organize the large  $N$  expansion as perturbation theory around the saddle point, by introducing the quantum fluctuation as

$$\Lambda_{\mathbf{n}} = \Lambda_0 + \tilde{\Lambda}_{\mathbf{n}}, \quad \Omega_{\mathbf{n}} = \Omega_0 + \tilde{\Omega}_{\mathbf{n}}, \quad (2.17)$$

together with  $J_{\mathbf{n}}^i = J_0^i + \tilde{J}_{\mathbf{n}}^i$ . In this paper we mainly consider up to 4-pt functions in the leading large  $N$  expansion and for this purpose it is sufficient to consider Gaussian fluctuations of fields. (A brief discussion on the 6-pt function will be presented later.) Using the saddle point equations (2.10) and (2.11), we expand the effective action as

$$\begin{aligned} S_{\text{eff}}(\Lambda, \Omega, J) &= S_{\text{eff}}(\Lambda_0, \Omega_0, J) + \sum_{\mathbf{n}} \left[ T_{\mathbf{n}}(\tilde{J}) i \tilde{\Lambda}_{\mathbf{n}} + \frac{1}{2} U''(\Omega_0) \tilde{\Omega}_{\mathbf{n}}^2 - i \tilde{\Lambda}_{\mathbf{n}} \tilde{\Omega}_{\mathbf{n}} \right] \\ &+ \sum_{\mathbf{nm}} \frac{1}{2} S_{\mathbf{nm}}(J) \tilde{\Lambda}_{\mathbf{n}} \tilde{\Lambda}_{\mathbf{m}} + \dots, \end{aligned} \quad (2.18)$$

where

$$T_{\mathbf{n}}(\tilde{J}) = \frac{1}{N} \sum_i \left[ (G \tilde{J}^i)_{\mathbf{n}} \right]^2 + \frac{2H}{\sqrt{NM^2}} (G \tilde{J}^N)_{\mathbf{n}}, \quad (2.19)$$

$$S_{\mathbf{nm}}(J) = 2G_{\mathbf{mn}}^2 + \frac{4}{N} \sum_i (G J^i)_{\mathbf{n}} G_{\mathbf{nm}} (G J^i)_{\mathbf{m}} \quad (2.20)$$

with

$$G_{\mathbf{nm}} \equiv (D^{-1}[\Lambda_0])_{\mathbf{nm}} = \frac{1}{V} \sum_{\mathbf{K}} G(\mathbf{K}) e^{i\mathbf{K}(n-m)}, \quad G(\mathbf{K}) = \frac{1}{\hat{\mathbf{K}}^2 + M^2}. \quad (2.21)$$

We then perform the Gaussian integral for  $\tilde{\Omega}_{\mathbf{n}}$  and  $\tilde{\Lambda}_{\mathbf{n}}$ , and finally obtain

$$Z(J) \simeq \mathcal{N}_3 \exp[-NW(J)] \quad (2.22)$$

where

$$W(J) = S_{\text{eff}}(\Lambda_0, \Omega_0, J) + \frac{1}{2} \sum_{\mathbf{nm}} T_{\mathbf{n}}(\tilde{J}) K_{\mathbf{nm}}^{-1}(J) T_{\mathbf{m}}(\tilde{J}) + \frac{1}{2N} \text{Tr} \ln K(J), \quad (2.23)$$

with

$$K_{nm}(J) = S_{nm}(J) + \frac{\delta_{nm}}{U'''(\Omega_0)}, \quad (2.24)$$

$$S_{\text{eff}}(\Lambda_0, \Omega_0, J) = V [U(\Omega_0) - U'(\Omega_0)\Omega_0] - \frac{1}{2} \text{Tr} \ln G - \frac{1}{2N} \sum_{nm,i} J_n^i G_{nm} J_m^i, \quad (2.25)$$

$$\mathcal{N}_3 = \mathcal{N}_2 \left( \frac{2\pi}{N\sqrt{U'''(\Omega_0)}} \right)^V = \left( \frac{(2\pi)^N}{U'''(\Omega_0)} \right)^{V/2}. \quad (2.26)$$

## 2.2 VEV and Correlation functions

We will call the first  $N-1$  components of  $\Phi$  "pions" and the  $N^{\text{th}}$  component "sigma", and denote  $\Pi_n^i = \Phi_n^i$  for  $i = 1, 2, \dots, N-1$  and  $\Sigma_n = \Phi_n^N$ , respectively. Taking derivatives of  $W(J)$  in eq. (2.22) with respect to the source  $J$  and setting  $J \rightarrow J_0$ , we can calculate the leading large  $N$  contributions to the connected part of arbitrary  $n$ -point functions.

We start with the vacuum expectation value (VEV) of  $\Sigma_n$  as

$$\begin{aligned} \sqrt{N}\Sigma &\equiv \langle \Sigma_n \rangle = \frac{-N\partial W(J)}{\partial J_n^N} \Big|_{J \rightarrow J_0} = \sqrt{N}H \sum_m G_{nm} - \frac{1}{2} \text{Tr} K^{-1}(J_0) \frac{\partial K(J)}{\partial J_n} \Big|_{J \rightarrow J_0}, \\ &= \sqrt{N} \frac{H}{M^2} \left[ 1 - \frac{4}{N} \sum_{lm} K_{lm}^{-1}(J_0) G_{ml} G_{mn} \right] = \sqrt{N} \frac{H}{M^2} \left[ 1 + O\left(\frac{1}{N}\right) \right], \end{aligned} \quad (2.27)$$

where

$$K_{nm}(J_0) = \frac{1}{V} \sum_{\mathbf{K}} e^{i\mathbf{K}(n-m)} \mathcal{K}(\mathbf{K}), \quad (2.28)$$

$$\mathcal{K}(\mathbf{K}) = \frac{1}{U'''(\Omega_0)} + 2J(\mathbf{K}) + \frac{4H^2}{M^4} G(\mathbf{K}), \quad (2.29)$$

$$J(\mathbf{K}) = \frac{1}{V} \sum_{\mathbf{Q}} G(\mathbf{Q}) G(\mathbf{K} + \mathbf{Q}). \quad (2.30)$$

The connected 2-pt function for  $\Pi$  is given by

$$\begin{aligned} \langle \Pi_n^i \Pi_m^j \rangle_c &\equiv \frac{-N\partial^2 W(J)}{\partial J_n^i \partial J_m^j} \Big|_{J \rightarrow J_0} = \delta^{ij} \left[ G_{nm} - \frac{4}{N} \sum_{ls} K_{sl}^{-1}(J_0) G_{nl} G_{ls} G_{sm} \right] \\ &= \delta^{ij} \left[ \frac{1}{V} \sum_{\mathbf{K}} G(\mathbf{K}) e^{i\mathbf{K}(n-m)} + O\left(\frac{1}{N}\right) \right], \end{aligned} \quad (2.31)$$

so that the pole mass of pions in lattice units becomes

$$M_\pi = 2 \sinh^{-1} \frac{M}{2}. \quad (2.32)$$

The connected 2-pt function for  $\Sigma$ , on the other hand, can be obtained as

$$\begin{aligned} \langle \Sigma_n \Sigma_m \rangle_c &\equiv \frac{-N\partial^2 W(J)}{\partial J_n^N \partial J_m^N} \Big|_{J \rightarrow J_0} = G_{nm} - \frac{4H^2}{M^4} \sum_{ls} G_{nl} K_{ls}^{-1}(J_0) G_{sm} + O\left(\frac{1}{N}\right), \\ &= \frac{1}{V} \sum_{\mathbf{K}} \Gamma_\Sigma^{(2)}(\mathbf{K}) e^{i\mathbf{K}(n-m)} + O\left(\frac{1}{N}\right) \end{aligned} \quad (2.33)$$

where

$$\Gamma_{\Sigma}^{(2)}(\mathbf{K}) = \frac{G(\mathbf{K})}{\mathcal{K}(\mathbf{K})} \left[ \mathcal{K}(\mathbf{K}) - \frac{4H^2}{M^4} G(\mathbf{K}) \right]. \quad (2.34)$$

The connected 4-pt function for  $\Pi$  is evaluated as<sup>1</sup>

$$\begin{aligned} \langle \Pi_{\mathbf{n}_1}^{i_1} \Pi_{\mathbf{n}_2}^{i_2} \Pi_{\mathbf{n}_3}^{i_3} \Pi_{\mathbf{n}_4}^{i_4} \rangle_c &\equiv \frac{-N \partial^4 W(J)}{\partial J_{\mathbf{n}_1}^{i_1} \partial J_{\mathbf{n}_2}^{i_2} \partial J_{\mathbf{n}_3}^{i_3} \partial J_{\mathbf{n}_4}^{i_4}} \Big|_{J \rightarrow J_0} \\ &= \frac{1}{V^3} \sum_{\mathbf{K}_1, \mathbf{K}_2, \mathbf{K}_3, \mathbf{K}_4} e^{i(\mathbf{K}_1 \mathbf{n}_1 + \mathbf{K}_2 \mathbf{n}_2 + \mathbf{K}_3 \mathbf{n}_3 + \mathbf{K}_4 \mathbf{n}_4)} \delta^{(3)}(\mathbf{K}_1 + \mathbf{K}_2 + \mathbf{K}_3 + \mathbf{K}_4) \frac{1}{N} \\ &\times G(\mathbf{K}_1) G(\mathbf{K}_2) G(\mathbf{K}_3) G(\mathbf{K}_4) \left[ \delta^{i_1 i_2} \delta^{i_3 i_4} \left\{ \Gamma_{\Pi}^{(4)}(\mathbf{K}_1 + \mathbf{K}_2) + O\left(\frac{1}{N}\right) \right\} + 2 \text{ perms} \right], \end{aligned} \quad (2.35)$$

where

$$\Gamma_{\Pi}^{(4)}(\mathbf{K}) = -4\mathcal{K}^{-1}(\mathbf{K}). \quad (2.36)$$

Similarly the connected 3-pt function for  $\Pi\Pi\Pi\Sigma$  is given by

$$\begin{aligned} \langle \Pi_{\mathbf{n}_1}^{i_1} \Pi_{\mathbf{n}_2}^{i_2} \Sigma_{\mathbf{n}_3} \rangle_c &\equiv \frac{-N \partial^3 W(J)}{\partial J_{\mathbf{n}_1}^{i_1} \partial J_{\mathbf{n}_2}^{i_2} \partial J_{\mathbf{n}_3}^N} \Big|_{J \rightarrow J_0} = \frac{1}{V^2} \sum_{\mathbf{K}_1, \mathbf{K}_2, \mathbf{K}_3} e^{i(\mathbf{K}_1 \mathbf{n}_1 + \mathbf{K}_2 \mathbf{n}_2 + \mathbf{K}_3 \mathbf{n}_3)} \\ &\times \delta^{(3)}(\mathbf{K}_1 + \mathbf{K}_2 + \mathbf{K}_3) \frac{1}{\sqrt{N}} G(\mathbf{K}_1) G(\mathbf{K}_2) G(\mathbf{K}_3) \left[ \delta^{i_1 i_2} \Gamma_{\Pi\Pi\Pi\Sigma}^{(3)}(\mathbf{K}_3) + O\left(\frac{1}{N}\right) \right] \end{aligned} \quad (2.37)$$

where

$$\Gamma_{\Pi\Pi\Pi\Sigma}^{(3)}(\mathbf{K}) = \frac{H}{M^2} \Gamma_{\Pi}^{(4)}(\mathbf{K}) = \Sigma \Gamma_{\Pi}^{(4)}(\mathbf{K}). \quad (2.38)$$

### 3 Renormalization and continuum limits

Let us consider the renormalization of this model in the leading large  $N$  for the infinite volume case, in order to take various continuum limits.

In the  $\mathbf{L} \rightarrow \infty$  limit the lattice sums discussed in the previous section become integrals:

$$I_{\infty}(M) = \int_{-\pi}^{\pi} \frac{d^3 \mathbf{K}}{(2\pi)^3} \frac{1}{\hat{\mathbf{K}}^2 + M^2}, \quad (3.1)$$

$$J_{\infty}(\mathbf{K}) = \int_{-\pi}^{\pi} \frac{d^3 \mathbf{Q}}{(2\pi)^3} \frac{1}{(\hat{\mathbf{Q}}^2 + M^2) \left[ (\widehat{\mathbf{K} + \mathbf{Q}})^2 + M^2 \right]}. \quad (3.2)$$

For small mass  $M \geq 0$  and small external momentum  $\mathbf{K}$ , we have

$$I_{\infty}(M) = I_0 - \frac{M}{4\pi} + I_2 M^2 + O(M^3), \quad (3.3)$$

$$J_{\infty}(\mathbf{K}) = \frac{1}{4\pi |\mathbf{K}|} \arctan\left(\frac{|\mathbf{K}|}{2M}\right) - I_2 + O(M, \mathbf{K}), \quad (3.4)$$

---

<sup>1</sup>Note that the lattice delta function we use here is periodic.



where constants  $I_0$  and  $I_2$  are numerically calculated as  $I_0 = 0.2527310\dots$  and  $I_2 = -0.0121641\dots$ .

There are two phases at  $H = 0$  in the infinite volume, the symmetric (SYM) phase where  $M^2 \neq 0$  and  $\Sigma = H/M^2 = 0$ , and the broken (BRO) phase where  $\Sigma \neq 0$  and  $M^2 = H/\Sigma = 0$ . Eqs. (2.13) and (2.14) at  $\Sigma = M = H = 0$  determine the phase boundary as  $3 = U'(I_0)$ .

We now solve the saddle point equations, eqs. (2.13) and (2.14) at  $H = 0$  near the continuum limit. In the SYM case, eqs. (2.13) and (2.14) become

$$I_0 - \frac{M}{4\pi} + I_2 M^2 + O(M^3) = \Omega_0, \quad 3 + \frac{M^2}{2} = U'(\Omega_0), \quad (3.5)$$

while in the BRO case, they are given by

$$I_0 + \Sigma^2 = \Omega_0, \quad 3 = U'(\Omega_0). \quad (3.6)$$

As can be seen later, it is convenient to define an effective 4-pt coupling constant  $u_{\text{eff}}$  as

$$U''(\Omega_0) = \frac{u_{\text{eff}}}{12} a, \quad (3.7)$$

where  $a$  is the lattice spacing. In the case of the  $\phi^4$  model,  $u_{\text{eff}} = U/a = g_4$ . We define the nonlinear  $\sigma$  model limit as the  $u_{\text{eff}} \rightarrow \infty$  limit.

### 3.1 Continuum limits in the symmetric phase

We first consider the SYM case. Defining the renormalized pion mass  $m_R$  as  $M = m_R a$  ( $m_R \geq 0$ ) with the lattice spacing  $a$  and expanding  $U'$  around  $I_0$  at  $O(a^2)$ , we obtain with eq. (3.7)

$$Z m_R^2 + \frac{u_{\text{eff}}}{24\pi} m_R - r_2 = O(a), \quad (3.8)$$

where we define

$$Z \equiv 1 - \frac{U'''(I_0)}{16\pi^2} \leq 1, \quad (3.9)$$

and make an additional tuning such that  $2U'(I_0) - 6 = r_2 a^2$ . We here restrict ourselves to the case that the effective 6-pt coupling  $U'''(I_0)$  is non-negative. As long as  $r_2 \geq 0$ , we obtain

$$m_R = \frac{\sqrt{u_{\text{eff}}^2 + 4(24\pi)^2 Z r_2} - u_{\text{eff}}}{48\pi Z}, \quad (3.10)$$

and  $r_2 = 0$  corresponds to the massless theory, while in the nonlinear  $\sigma$  model limit we have

$$m_R = \frac{24\pi r_2}{u_{\text{eff}}} \quad (3.11)$$

if  $r_2 = O(u_{\text{eff}})$ . Using  $m_R$ , the renormalized 2-pt function in the momentum space is given by

$$\gamma_\pi^{(2)}(\mathbf{k}) = \frac{1}{\mathbf{k}^2 + m_R^2}. \quad (3.12)$$

Instead of the dimensional parameter  $r_2$ , we use the renormalize pion mass  $m_R$ , in addition to the dimensional coupling  $u_{\text{eff}}$ , in order to specify the continuum limit. Then  $r_2$  is expressed by others as

$$r_2 = Zm_R^2 \left( 1 + \frac{1}{24\pi Z\alpha} \right) \geq 0 \quad (3.13)$$

in the symmetric phase, where we introduce the ratio  $\alpha = m_R/u_{\text{eff}}$ . We call a massive theory ( $m_R \neq 0$ ) case A and a massless theory ( $m_R = 0$ ) case B, while the nonlinear  $\sigma$  model limit is named as case I and otherwise as case II, so that there are four different continuum limits, IA, IB, IIA, IIB.

We next define the renormalized 4-pt vertex function in the symmetric phase as

$$\gamma_\pi^{(4)}(\mathbf{k}) = \frac{\Gamma_{\text{II}}^{(4)}(\mathbf{K} = \mathbf{ka})}{a} \rightarrow -\frac{1}{3} \frac{u_{\text{eff}}}{1 + \frac{u_{\text{eff}}}{24\pi|\mathbf{k}|} \arctan\left(\frac{|\mathbf{k}|}{2m_R}\right)}, \quad (3.14)$$

where we use the effective coupling defined in eq. (3.7).

We define a line of constant physics (LCP) by a curve on which  $\alpha \equiv m_R/u_{\text{eff}}$  is kept constant even at finite lattice spacing. Taking  $G = G_{k \geq 4} = 0$  for simplicity, the LCP is determined by

$$\frac{R}{2} = 3 + \frac{\alpha^2 U^2}{2} - \frac{U}{12} I_\infty(\alpha U). \quad (3.15)$$

In Fig. 1, we draw this LCP at several values of  $\alpha$  in the  $(U, R)$  plane.

### 3.2 Continuum limits in the broken phase

In the broken phase, using the saddle point equation in the  $H \rightarrow 0$  limit, we obtain the renormalized condensate  $\sigma_R^2 = \Sigma^2/a$  in the continuum limit as

$$\sigma_R^2 \equiv w_R = \begin{cases} \frac{u_{\text{eff}}}{12Z_B} \left( 1 - \sqrt{1 + r_2 Z_B \left( \frac{12}{u_{\text{eff}}} \right)^2} \right), & Z_B \equiv U'''(I_0) > 0 \\ -6 \frac{r_2}{u_{\text{eff}}} & Z_B = 0 \end{cases}. \quad (3.16)$$

Therefore  $r_2$  must be negative in the broken phase. We call the broken phase the case C, and there are IC and IIC depending on  $u_{\text{eff}}$ .

The renormalized 4-pt vertex function in the continuum limit is given by

$$\gamma_\pi^{(4)}(\mathbf{k}) = -\frac{1}{3} \frac{u_{\text{eff}}}{1 + \frac{u_{\text{eff}}}{48|\mathbf{k}|} + \frac{w_R u_{\text{eff}}}{3\mathbf{k}^2}}, \quad (3.17)$$

which is related to the  $\pi\pi\sigma$  3-pt vertex function in the continuum limit as

$$\gamma_{\pi\pi\sigma}^{(3)}(\mathbf{k}) \equiv \frac{\Gamma_{\text{III}\Sigma}^{(3)}(\mathbf{K} = \mathbf{ka})}{a^{3/2}} = \sqrt{w_R} \gamma_\pi^{(4)}(\mathbf{k}). \quad (3.18)$$

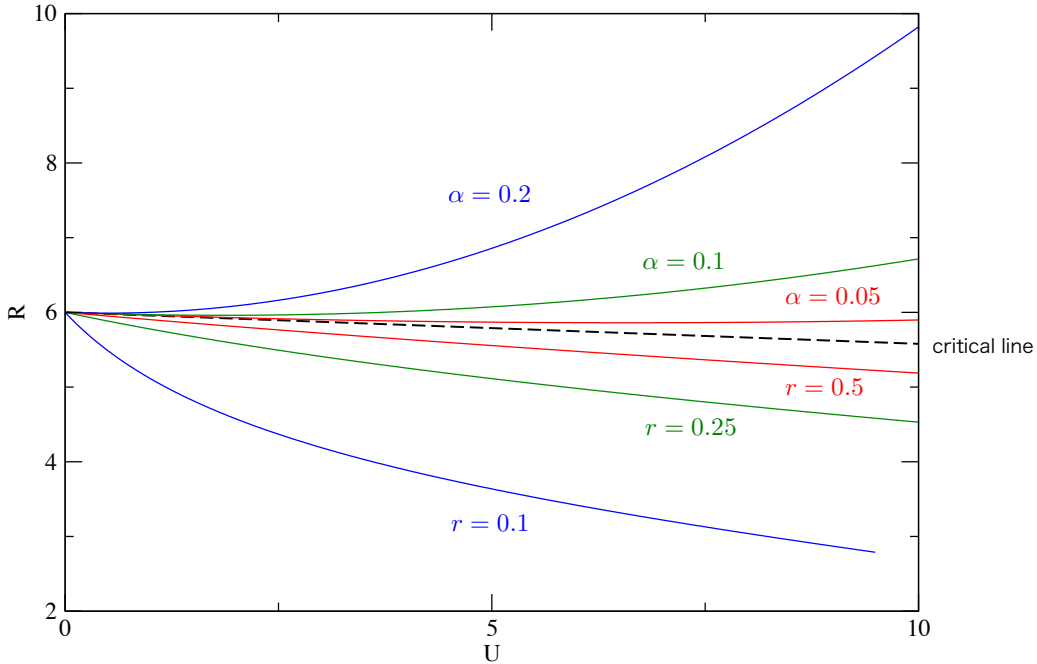


**Figure 1.** Lines of constant physics for  $G = G_{k \geq 4} = 0$ . The dashed black line is the critical line. In the symmetric phase (above the critical line) the red, green and blue curves are lines of constant  $\alpha = 0.05, 0.1, 0.2$  respectively. In the broken phase the red, green and blue curves are lines of constant  $r = 0.5, 0.25, 0.1$  respectively.

Finally the continuum limit of the connected 2-pt function for  $\sigma$  is given by

$$\gamma_\sigma^{(2)}(\mathbf{k}) = a^2 \Gamma_\Sigma^{(2)}(\mathbf{K} = \mathbf{k}a) = \frac{1 + \frac{u_{\text{eff}}}{48|\mathbf{k}|}}{\mathbf{k}^2 + \frac{u_{\text{eff}}}{48}|\mathbf{k}| + \frac{w_R u_{\text{eff}}}{3}}, \quad (3.19)$$

which has a pole at

$$|\mathbf{k}| = \gamma(-1 \pm \sqrt{1 - 64\beta}), \quad \gamma = \frac{u_{\text{eff}}}{96}, \quad \beta = 48 \frac{w_R}{u_{\text{eff}}}, \quad (3.20)$$

while the pion is massless in this phase. If we interpret  $|\mathbf{k}|$  as  $\sqrt{-k_0^2 + k_1^2 + k_2^2}$  and taking  $k_0 = m_\sigma - i\Gamma_\sigma$ ,  $k_1 = k_2 = 0$ , we obtain

$$-k_0^2 = -(m_\sigma^2 - \Gamma_\sigma^2) + 2im_\sigma\Gamma_\sigma = 2\gamma^2 \left[ 1 - 32\beta \mp \sqrt{1 - 64\beta} \right]. \quad (3.21)$$

If  $0 \leq \beta < 1/64$ ,  $-k_0^2$  is real and positive, so that there is no pole in the propagator. On the other hand, if  $1/64 \leq \beta$ , we have the  $\sigma$  resonance, whose mass and width are given by

$$m_\sigma^2 = \gamma^2(64\beta - 1), \quad \Gamma_\sigma^2 = \gamma^2. \quad (3.22)$$

In Fig. 1 we have also plotted lines of constant  $r \equiv \Gamma_\sigma/m_\sigma$  (the ratio of resonance width over mass) for the lattice regularization with  $G = G_{k \geq 4} = 0$ . For technical details we refer to Appendix A. At  $U \sim 10$  on the lines for  $r = 0.5, 0.25, 0.1$ , the values of the lattice mass  $M_\sigma$  are  $\sim 0.20, 0.41, 1.0$ . Lattice artifacts for the ratio  $\Sigma^2/M_\sigma$  are rather small along these lines (in the region plotted), only deviating maximally a few percent from the continuum limit  $\omega_R/m_\sigma = (r + 1/r)/32$ .

### 3.3 6-pt vertex function for $\pi$ fields

We can also calculate the 6-pt vertex function for  $\pi$  fields, by considering the third order of quantum fluctuation in eq. (2.18) as

$$U'''(\Omega_0) \sum_{\mathbf{n}} \frac{\tilde{\Omega}_{\mathbf{n}}^3}{3!} - \frac{4i}{3} \sum_{\mathbf{n}_1, \mathbf{n}_2, \mathbf{n}_3} G_{\mathbf{n}_1 \mathbf{n}_2} G_{\mathbf{n}_2 \mathbf{n}_3} G_{\mathbf{n}_3 \mathbf{n}_1} \tilde{\Lambda}_{\mathbf{n}_1} \tilde{\Lambda}_{\mathbf{n}_2} \tilde{\Lambda}_{\mathbf{n}_3} \quad (3.23)$$

at the leading order of the large  $N$  expansion.

The connected 6-pt function for  $\pi$  in the continuum limit is  $O(1/N^2)$ , and is given in the momentum space as

$$\delta^{(3)}\left(\sum_{i=1}^6 \mathbf{k}_i\right) \prod_{i=1}^6 \gamma_\pi^{(2)}(\mathbf{k}_i) \times \frac{1}{N^2} \left[ \left\{ \gamma_\pi^{(6),1PI}(\mathbf{k}_{12}, \mathbf{k}_{34}) \delta_{i_1 i_2} \delta_{i_3 i_4} \delta_{i_5 i_6} + 14 \text{ perms} \right\} \right. \\ \left. + \left\{ \gamma_\pi^{(6),1PR}(\mathbf{k}_{12}, \mathbf{k}_{123}, \mathbf{k}_{56}) \delta_{i_1 i_2} \delta_{i_3 i_4} \delta_{i_5 i_6} + 89 \text{ perms} \right\} \right] \quad (3.24)$$

where  $\mathbf{k}_{ij} = \mathbf{k}_i + \mathbf{k}_j$ ,  $\mathbf{k}_{ijk} = \mathbf{k}_i + \mathbf{k}_j + \mathbf{k}_k$ , and the 1-particle irreducible(1PI) 6-pt vertex function is given by

$$\gamma_\pi^{(6),1PI}(\mathbf{k}, \mathbf{p}) = \gamma_\pi^{(4)}(\mathbf{k}) \gamma_\pi^{(4)}(\mathbf{p}) \gamma_\pi^{(4)}(\mathbf{k} + \mathbf{p}) \left[ \frac{U'''(I_0)}{(u_{\text{eff}}/6)^3} + T(\mathbf{k}, -\mathbf{p}) \right], \quad (3.25)$$

$$T(\mathbf{k}, -\mathbf{p}) = \int \frac{d^3 q}{(2\pi)^3} \gamma_\pi^{(2)}(\mathbf{q}) \gamma_\pi^{(2)}(\mathbf{q} + \mathbf{k}) \gamma_\pi^{(2)}(\mathbf{q} - \mathbf{p}) \\ = \frac{1}{16\pi} \int_0^1 dx \int_0^1 dy \frac{y}{[m_R^2 + f(x, y, \mathbf{k}, \mathbf{p})]^{3/2}} \quad (3.26)$$

with  $f(x, y, \mathbf{k}, \mathbf{p}) = \mathbf{k}^2 xy(1-xy) + \mathbf{p}^2 y(1-y) + 2\mathbf{k} \cdot \mathbf{p} xy(1-y)$ , while the 1-particle reducible (1PR) 6-pt vertex function becomes

$$\gamma_\pi^{(6),1PR}(\mathbf{k}, \mathbf{p}, \mathbf{q}) = \gamma_\pi^{(4)}(\mathbf{k}) \gamma_\pi^{(2)}(\mathbf{p}) \gamma_\pi^{(4)}(\mathbf{q}). \quad (3.27)$$

Note that the term in eq. (3.27) and the second term in eq. (3.25) are generated by the 4-pt vertex. Since the theory is super-renormalizable without bare 6-pt coupling, however, they do not generate any UV divergences once  $m_R$  (or  $w_R$ ) and  $u_{\text{eff}}$  are made finite in the continuum limit. Therefore the effective 6-pt coupling  $U'''(I_0)$  is not required to renormalize the theory, so that it can take an arbitrary non-negative value including zero.

The contribution from  $U'''(I_0)$  to the 8-pt vertex function, on the other hand, vanishes in the continuum limit, showing that it corresponds to the non-renormalizable coupling in the continuum theory.

## 4 Running four-point coupling

Our definition of the running coupling  $g_4$  is

$$g_4(\mathcal{E}) \equiv -\frac{3\gamma_\pi^{(4)}(|\mathbf{k}| = \mathcal{E})}{\mathcal{E}}. \quad (4.1)$$

This means that we measure the dimensionful four-point vertex function in units of the energy scale at which it is measured. Our results crucially depend on this definition, which we however found natural. Also this is the definition that gives identically vanishing beta function for the conformal model, as required.

There are six different continuum limits, A (massive symmetric), B (massless symmetric) and C (broken) times I (finite  $u_{\text{eff}}$ ) and II ( $u_{\text{eff}} \rightarrow \infty$ ). The corresponding running coupling is given as follows (with  $m_R > 0$ ).

$$\begin{aligned} \text{case IA : } \quad g_4(\mathcal{E}) &= \frac{24\pi}{\arctan(\mathcal{E}/2m_R)}, & g_4(0) &= \infty, & g_4(\infty) &= 48 \\ \text{case IB : } \quad g_4(\mathcal{E}) &= 48 \\ \text{case IIA : } \quad g_4(\mathcal{E}) &= \frac{24\pi}{24\pi\mathcal{E}\alpha/m_R + \arctan(\mathcal{E}/2m_R)}, & g_4(0) &= \infty, & g_4(\infty) &= 0 \\ \text{case IIB : } \quad g_4(\mathcal{E}) &= \frac{48}{1 + 48\mathcal{E}/u_{\text{eff}}}, & g_4(0) &= 48, & g_4(\infty) &= 0 \\ \text{case IC : } \quad g_4(\mathcal{E}) &= \frac{48\mathcal{E}/w_R}{16 + \mathcal{E}/w_R}, & g_4(0) &= 0, & g_4(\infty) &= 48 \\ \text{case IIC : } \quad g_4(\mathcal{E}) &= \frac{48\mathcal{E}/w_R}{16 + \mathcal{E}/w_R + 48\mathcal{E}^2/(w_R u_{\text{eff}})}, & g_4(0) &= 0, & g_4(\infty) &= 0 \end{aligned} \quad (4.2)$$

We see that case IB is conformal:  $g_4 \equiv 48$ . Case IA is Ultra-Violet (UV) conformal, the range of  $g_4$  is from  $\infty$  to 48 as we move from Infra-Red (IR) to UV. For case IIA the range is from  $\infty$  to 0 and thus it is an UV Asymptotically Free (AF) model. For IIB the range of  $g_4$  is from 48 to 0, this limiting model is UV AF and conformal in the IR. In the broken phase case, IC can be called UV conformal again since  $g_4$  grows from 0 to 48 and finally for the generic broken phase case IIC  $g_4$  grows from 0 to a  $\beta$ -dependent maximum value at  $\mathcal{E}^2 = w_R u_{\text{eff}}/3$  and then decreases again to 0.

The generic case IIA is our toy model for YM theory and IIB corresponds to the case where there is also an IR fixed point. For IIA and small  $\alpha$ , the theory is “walking” in the region around  $g_4 \approx 48$ .

### 4.1 Beta function

We take the usual definition

$$\beta_4(g_4) = \mathcal{E} \frac{\partial}{\partial \mathcal{E}} g_4(\mathcal{E}). \quad (4.3)$$

Let us first consider the symmetric case. The beta function is always negative here (except for the conformal case IB, where it is identically vanishing). For IA we have

$$\beta_4(g_4) = -\frac{g_4^2}{48\pi} \sin(48\pi/g_4), \quad (4.4)$$

while for IIB

$$\beta_4(g_4) = -g_4 + \frac{g_4^2}{48}. \quad (4.5)$$

For the generic case IIA the beta function can be implicitly given by first solving

$$\frac{2}{\pi} \arctan \xi + b\xi = \frac{48}{g_4} \quad (4.6)$$

for the variable  $\xi$ , where  $b = 96\alpha$ . The beta function is then

$$\beta_4(g_4) = -g_4 + \frac{g_4^2}{24\pi} \left( \arctan \xi - \frac{\xi}{1 + \xi^2} \right). \quad (4.7)$$

For small coupling we have the expansion

$$\beta_4(g_4) = -g_4 + \frac{g_4^2}{48} - \frac{\alpha g_4^3}{6\pi} + \dots \quad (4.8)$$

It is interesting to note that (4.5) are the first two terms of the weak coupling expansion of the beta function  $\beta_4$  for any  $\alpha$  in case IIA. For this generic case we can calculate the beta function numerically. It depends on the parameter  $b$ . Fig. 2 shows the beta function for  $b = 96\alpha = 0.119, 0.0119$  and  $0.00119$ . They nicely show the walking behaviour for small  $\alpha$ : the beta function is close to (4.5) for  $0 < g_4 < 48$ , and to (4.4) for  $48 < g_4 < \infty$ . We note that it is necessary to go extremely close to the conformal point  $\alpha = 0$  to be able to observe “walking” of the beta function.

In the broken phase (in the generic case IIC) the beta function is a double valued function of the coupling:

$$\beta_4(g_4) = \pm \frac{g_4}{48} \sqrt{(48 - g_4)^2 - 64\beta g_4^2} = \pm \left\{ g_4 - \frac{g_4^2}{48} - \frac{\beta g_4^3}{72} + \dots \right\}. \quad (4.9)$$

The coupling has finite range:

$$0 \leq g_4 \leq \frac{48}{1 + 8\sqrt{\beta}} \quad (4.10)$$

and the beta function is

$$\text{positive for } 0 < \mathcal{E} < \frac{4w_R}{\sqrt{\beta}}, \quad \text{negative for } \frac{4w_R}{\sqrt{\beta}} < \mathcal{E}. \quad (4.11)$$

For case IC the beta function is positive:

$$\beta_4(g_4) = g_4 - \frac{g_4^2}{48}. \quad (4.12)$$

## 4.2 Lattice artifact and finite size corrections to the “walking” behavior of the beta function

In the case IIA, the running coupling in the continuum limit on the infinite volume is given by

$$g_4(\mathcal{E}) = \frac{1}{x + \frac{1}{24\pi} \arctan \left( \frac{x}{2\alpha} \right)} \quad (4.13)$$

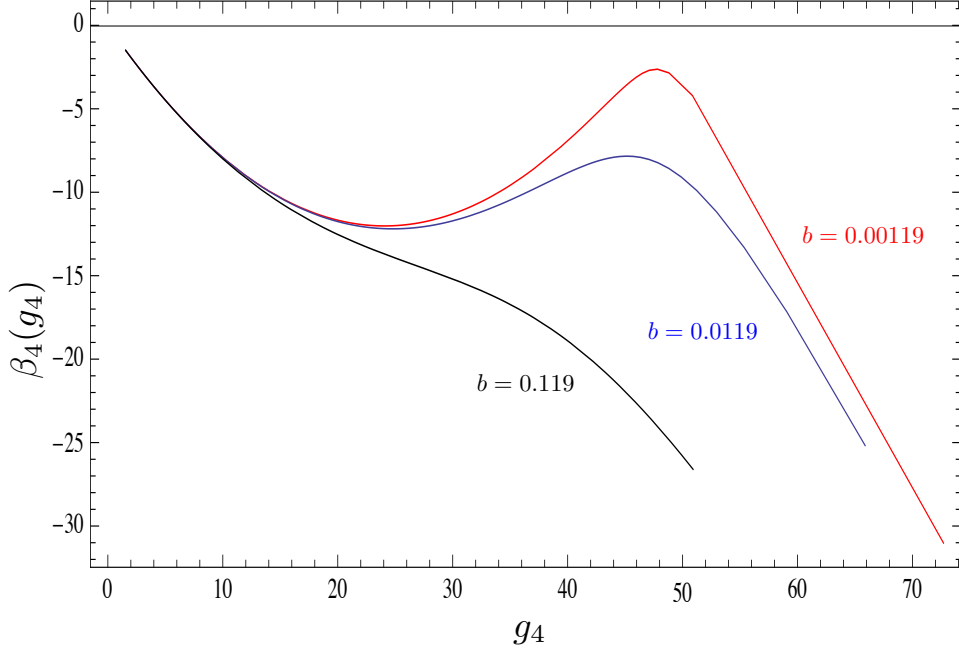


**Figure 2.** The beta function in the symmetric phase for  $b = 0.119$  (black),  $0.0119$  (blue) and  $0.00119$  (red).

where  $x = \mathcal{E}/u_{\text{eff}}$ . In this subsection, we consider an effect of non-zero  $a$  and finite volume to the beta function. For simplicity of analysis, we set  $G = G_{k \geq 4} = 0$ , and then introduce the lattice spacing through  $U$  as  $U = u_{\text{eff}}a$ . The running coupling thus becomes

$$g_4^{\text{lat}}(\mathbf{K}) = \frac{1}{x + \frac{x}{6}UJ(\mathbf{K})} \quad (4.14)$$

where

$$\begin{aligned} UJ(\mathbf{K}) &= \frac{U}{L_0 L_1 L_2} \sum_{l_{0,1,2}=0}^{L_{0,1,2}-1} \frac{1}{[\widehat{\mathbf{Q}}^2 + \alpha^2 U^2] \left[ (\widehat{\mathbf{K} + \mathbf{Q}})^2 + \alpha^2 U^2 \right]} \\ &= \prod_{i=0}^2 \frac{1}{L_i U} \sum_{l_{0,1,2}=0}^{L_{0,1,2}-1} \frac{1}{[\widehat{\mathbf{q}}^2 + \alpha^2] \left[ (\widehat{\mathbf{k} + \mathbf{q}})^2 + \alpha^2 \right]}, \end{aligned} \quad (4.15)$$

$$\mathbf{Q} = 2\pi \left( \frac{l_0}{L_0}, \frac{l_1}{L_1}, \frac{l_2}{L_2} \right) = \mathbf{q}U, \quad \mathbf{K} = 2\pi \left( \frac{n_0}{L_0}, \frac{n_1}{L_1}, \frac{n_2}{L_2} \right) = \mathbf{k}U \quad (4.16)$$

with  $\mathbf{k}^2 = x^2$ .

In Fig. 3, we compare the beta function of  $g_4^{\text{lat}}$  with that of  $g_4$  as a function of  $g_4$  in the symmetric phase at  $b = 0.0119$ , where the "walking" behavior is clearly seen in the continuum limit (the black line). We take  $\mathbf{K} = (K_0, 0, 0)$  with  $0 \leq K_0 \leq \pi$  in this calculation. In the figure, the solid lines show the behavior of the beta function in the infinite volume at finite lattice spacing, corresponding to  $m_R a = 0.005$  (magenta), 0.05 (red), 0.1 (green) and 0.2 (blue), where  $U = 96 m_R a / b$ . As  $a$  increases, the lattice beta function deviates from its continuum one, in particular at small  $g_4$ , where the energy scale  $x$  becomes large due to the asymptotic freedom. We however still can observe the "walking" behavior around  $g_4 \simeq 48$ . In the finite volume case, we take  $L_0 = L_1 = L_2 = L$  for simplicity. Instead of the derivative, we use the symmetric difference of the discrete energy  $x$  in the finite volume to define the lattice beta function. In the figure, symbols represent the beta function at  $L = 30$  (diamonds), 40 (squares) and 80 (circles) at  $m_R a = 0.1$  (green) while  $L = 15$  (diamonds), 20 (squares) and 40 (circles) at  $m_R a = 0.2$  (blue), which give  $m_R a L = 3, 4$  and 8 for both cases. We observe that the finite size effect to the beta function is rather mild, except at strong coupling in the low energy region.

## 5 Scattering phase shifts

### 5.1 Scattering amplitude

The pion scattering amplitude in the large  $N$  limit is given by

$$T^{i_1 i_2, i_3 i_4}(\mathbf{k}_1, \mathbf{k}_2 | \mathbf{k}_3, \mathbf{k}_4) \equiv \lim_{\mathbf{k}_{1,2,3,4} \rightarrow \text{on-shell}, \sum_i \mathbf{k}_i = 0} \frac{1}{N-1} \left[ \delta^{i_1 i_2} \delta^{i_3 i_4} \gamma_\pi^{(4)}(\mathbf{k}_1 + \mathbf{k}_2) + 2 \text{ perms} \right], \quad (5.1)$$

where on-shell momenta in the center of mass system are given by  $\mathbf{k}_1 = (iE_p, \vec{p})$ ,  $\mathbf{k}_2 = (iE_p, -\vec{p})$ ,  $\mathbf{k}_3 = (-iE_q, \vec{q})$ ,  $\mathbf{k}_4 = (-iE_q, -\vec{q})$  with  $E_p^2 = \vec{p}^2 + m_R^2 = E_q^2 = \vec{q}^2 + m_R^2$ ,  $\vec{p} = (p_1, p_2)$  and  $\vec{q} = (q_1, q_2)$ . Explicitly we have

$$T^{i_1 i_2, i_3 i_4}(\mathbf{k}_1, \mathbf{k}_2 | \mathbf{k}_3, \mathbf{k}_4) = \frac{1}{N-1} \left[ \delta^{i_1 i_2} \delta^{i_3 i_4} \gamma_\pi^{(4)}(2iE_p, \vec{0}) + \delta^{i_1 i_3} \delta^{i_2 i_4} \gamma_\pi^{(4)}(0, \vec{p} + \vec{q}) + \delta^{i_1 i_4} \delta^{i_3 i_2} \gamma_\pi^{(4)}(0, \vec{p} - \vec{q}) \right]. \quad (5.2)$$

In terms of the "isospin" decomposition for  $N-1$  pions

$$T^{i_1 i_2, i_3 i_4}(\mathbf{k}_1, \mathbf{k}_2 | \mathbf{k}_3, \mathbf{k}_4) = \sum_{I=0}^2 Q_I^{i_1 i_2, i_3 i_4} T_I(\vec{p}, \vec{q}) \quad (5.3)$$

with projectors

$$Q_0^{i_1 i_2, i_3 i_4} = \frac{1}{N-1} \delta^{i_1 i_2} \delta^{i_3 i_4}, \quad (5.4)$$

$$Q_1^{i_1 i_2, i_3 i_4} = \frac{1}{2} (\delta^{i_1 i_3} \delta^{i_2 i_4} - \delta^{i_1 i_4} \delta^{i_2 i_3}), \quad (5.5)$$

$$Q_2^{i_1 i_2, i_3 i_4} = \frac{1}{2} (\delta^{i_1 i_3} \delta^{i_2 i_4} + \delta^{i_1 i_4} \delta^{i_2 i_3}) - \frac{1}{N-1} \delta^{i_1 i_2} \delta^{i_3 i_4}, \quad (5.6)$$



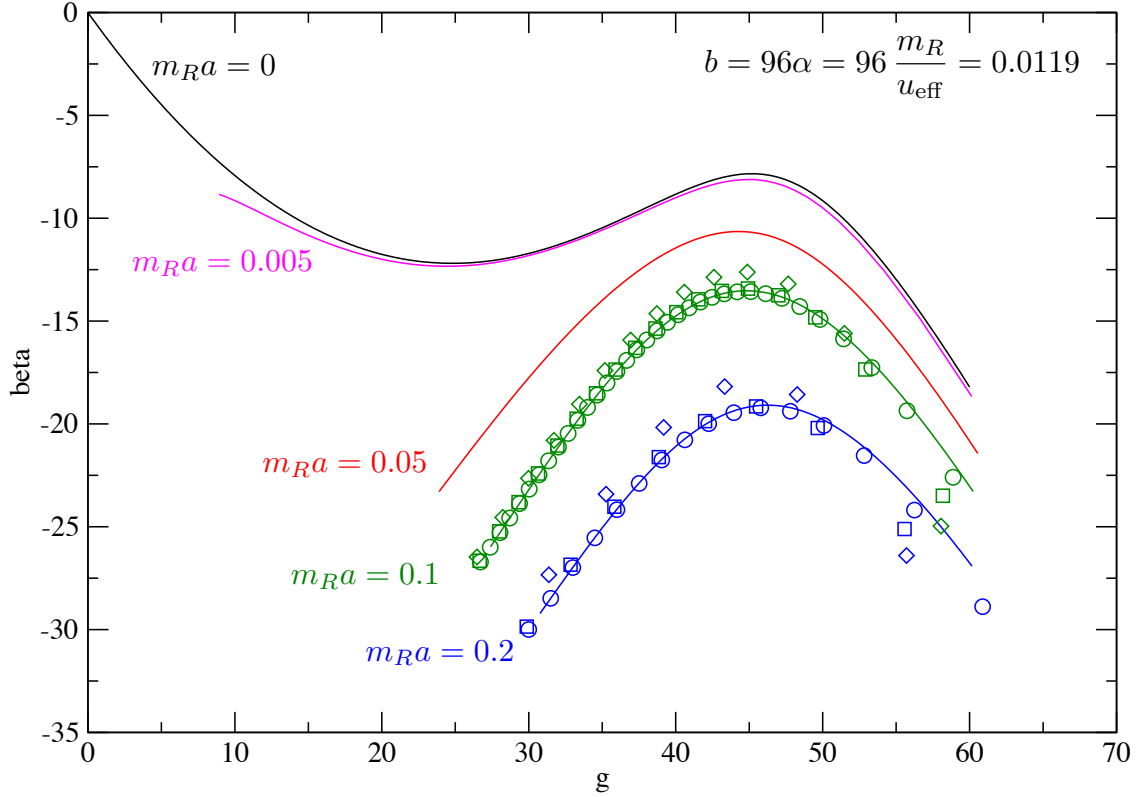


**Figure 3.** The beta function in the symmetric phase at  $b = 0.0119$  for several values of lattice spacings and the volume. For further details please consult the text.

we obtain

$$T_0(\vec{p}, \vec{q}) = \gamma_\pi^{(4)}(2iE_p, \vec{0}) + \frac{1}{N-1} \left[ \gamma_\pi^{(4)}(0, \vec{p} + \vec{q}) + \gamma_\pi^{(4)}(0, \vec{p} - \vec{q}) \right], \quad (5.7)$$

$$T_1(\vec{p}, \vec{q}) = \frac{1}{N-1} \left[ \gamma_\pi^{(4)}(0, \vec{p} + \vec{q}) - \gamma_\pi^{(4)}(0, \vec{p} - \vec{q}) \right], \quad (5.8)$$

$$T_2(\vec{p}, \vec{q}) = \frac{1}{N-1} \left[ \gamma_\pi^{(4)}(0, \vec{p} + \vec{q}) + \gamma_\pi^{(4)}(0, \vec{p} - \vec{q}) \right]. \quad (5.9)$$

Therefore, in the large  $N$  limit, we have

$$T_0(\vec{p}, \vec{q}) = \lim_{\varepsilon \rightarrow 0} \gamma_\pi^{(4)}((i - \varepsilon)W, \vec{0}), \quad T_1(\vec{p}, \vec{q}) = T_2(\vec{p}, \vec{q}) = 0, \quad (5.10)$$

where  $W = 2E_p$ .

Using the integral formula in the continuum limit

$$\lim_{a \rightarrow 0} \lim_{\varepsilon \rightarrow 0} aJ \left( (i - \varepsilon)W a, \vec{0} \right) = \frac{1}{4\pi W} \operatorname{arccoth} \left( \frac{W}{2m_R} \right) + i \frac{1}{8W}, \quad (5.11)$$

we have

$$T_0(\vec{p}, \vec{q}) = -\frac{1}{X + iY}, \quad (5.12)$$

where

$$X = \begin{cases} \frac{3}{u_{\text{eff}}} + \frac{1}{8\pi W} \operatorname{arccoth} \left( \frac{W}{2m_R} \right), & \text{SYM} \\ \frac{3}{u_{\text{eff}}} - \frac{w_R}{W^2}, & \text{BRO} \end{cases}, \quad Y = \frac{1}{16W}. \quad (5.13)$$

## 5.2 Unitarity and scattering phase shift

The scattering amplitude  $T_0$  in eq. (5.12) satisfies unitarity

$$i \left[ T_0 - T_0^\dagger \right] (\vec{p}, \vec{q}) = -\frac{1}{2W} \int \frac{d^2k}{(2\pi)^2} \frac{1}{2E_k} (2\pi) \delta(W - 2E_k) T_0(\vec{p}, \vec{k}) T_0^\dagger(\vec{k}, \vec{q}), \quad (5.14)$$

where  $E_k^2 = \vec{k}^2 + m_R^2$ . Therefore,  $T_0$  can be expressed as

$$T_0(\vec{p}, \vec{q}) = 16W e^{i\delta_0(W)} \sin \delta_0(W) \quad (5.15)$$

where  $\delta_0(W)$  is the scattering phase shift for the  $I = 0$  channel, so that we obtain

$$\cot \delta_0(W) = -\frac{X}{Y} = \begin{cases} -\frac{48W}{u_{\text{eff}}} - \frac{2}{\pi} \operatorname{arccoth} \left( \frac{W}{2m_R} \right), & \text{SYM} \\ -\frac{48W}{u_{\text{eff}}} + \frac{16w_R}{W}, & \text{BRO} \end{cases}. \quad (5.16)$$

Fig. 4 shows behaviors of  $\delta_0(W)$  as a function of  $W$  in the symmetric phase, which clearly reflect behaviors of the running coupling in the various continuum limits: In the case IA given by the dashed line,  $\delta_0(W)$  starts from 0 at  $W = 0$  and monotonically approaches  $-\pi/2$  as  $W$  increases.  $\delta_0(W) = -\pi/2$  is the value for the conformal theory, as shown by the solid magenta line corresponding to the case IB. This shows that the case IA is UV conformal. The behavior of  $\delta_0(W)$  in the general case IIA depends on the mass, namely on the parameter  $b = 96\alpha = 96m_R/u_{\text{eff}}$ . At relatively large  $m_R$  ( $b = 1.19$ ) denoted by the solid black line,  $\delta_0(W)$  first decreases from 0 as  $W$  increases but, at some value of  $W$ , it starts to increase toward 0, showing that the IIA case is asymptotically free in the UV. If we decrease  $m_R$  ( $b = 0.00119$ ),  $\delta_0(W)$  rapidly decreases from 0 to  $-\pi/2$  (the conformal value) near  $W = 0$  and gradually increases toward 0 for increasing  $W$ , as shown by the solid red line. In the case of the massless limit, the case IIB,  $\delta_0(W) = -\pi/2$  at  $W = 0$  and monotonically increases toward 0, showing the theory is IR conformal and UV

asymptotically free. The IIA case with small mass such as  $b = 0.00119$  is nearly conformal, and therefore has "walking" coupling.

This shows that, although the running coupling is not a physical observable and depends on how it is defined, it captures some properties of the scattering phase shift. In other words, it opens a possibility to identify a nearly conformal theory (or the walking coupling) unambiguously from the physical observable, the scattering phase shift.

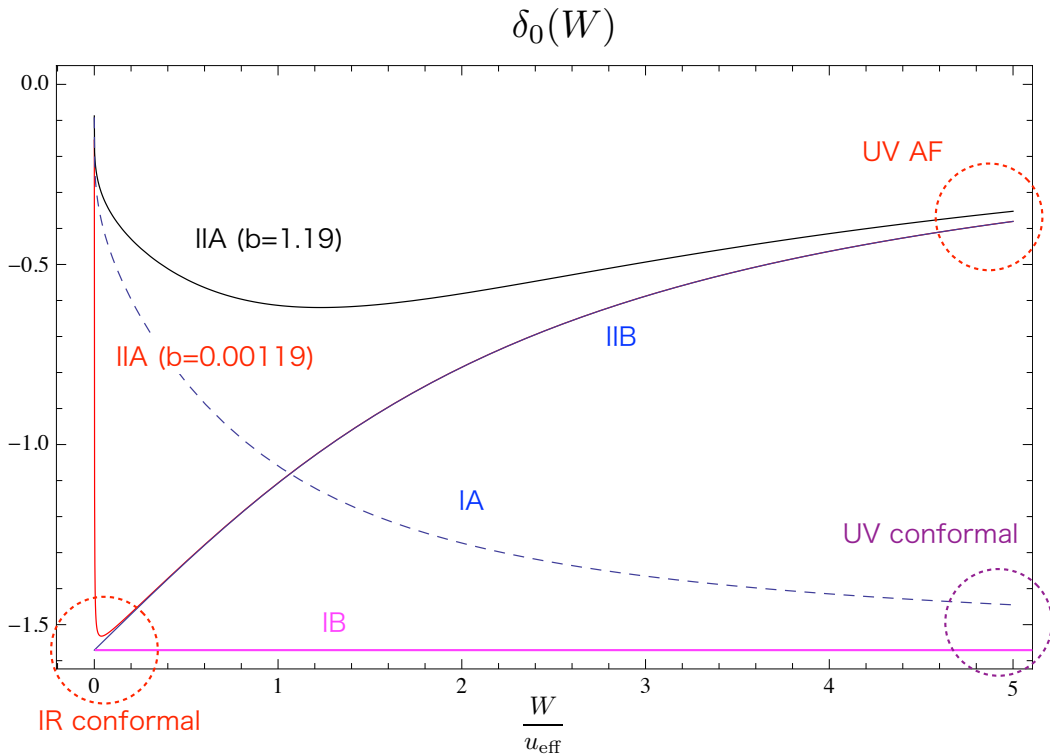


**Figure 4.** Scattering phase shift  $\delta_0(W)$  as a function of  $W/u_{\text{eff}}$  for IA(dashed line), IB(solid magenta line), IIA with  $\cong 96\alpha = 1.19$  (solid black line), IIA with  $b = 0.00119$  (solid red line) and IIB (solid blue line).

## 6 Summary

Due to the difficulties in establishing walking behavior in candidate models in 4-dimensions using lattice simulations, it is helpful to have simple toy models which show this phenomenon and where the problematic systematic errors can be investigated in detail. Although some features discovered in such models may be quite different in realistic models, such studies may give some valuable insights and indications where caution should be applied.

With this motivation we have shown that the  $O(N)$  scalar field theory in 3 dimensions exhibits walking behavior in the large  $N$  limit when a continuous parameter  $\alpha = m_R/u_{\text{eff}}$ ,

the ratio of renormalized mass to an effective 4-point coupling (with dimension mass), is very small. The characteristic walking, a slow change in dynamical behavior over a range of (low) energies, has been demonstrated for various couplings defined in infinite and finite volumes and also for the (on-shell) scattering phase shift, as well as asymptotic freedom at high energies.

Some potential problems for lattice simulations were identified. Firstly we have seen that (in the symmetric phase) for  $\alpha$  in the range where walking sets in, it would, for infinite volume couplings, be practically extremely difficult to reach energies where asymptotic freedom sets in. Recursive finite size scaling methods would certainly help in this respect.

Secondly although a qualitative characteristic of walking behavior, a maximum of the beta function at some non-zero value of the coupling, is observed at moderate correlation lengths, quantitative conclusions are marred by large lattice artifacts. The additional finite volume effects at medium energies are not so large and do not distort the results provided  $m_R L \geq 3$ .

The toy model in the broken phase exhibits also rather interesting dynamics, which remains to be explored in detail. In particular it manifests a resonance, and various continuum limits are characterized by values of  $r = \Gamma_\sigma/m_\sigma$ , the ratio of the width to the resonance mass. Again here systematic sources of errors associated with the lattice regularization can be studied. For example along lines of constant physics defined through keeping  $r$  fixed, we have found that lattice artifacts in the ratio of the vacuum expectation value squared to the mass are rather small for correlation lengths  $> \sim 2$ .

## Acknowledgement

S. A. is supported in part by the Grant-in-Aid of the Japanese Ministry of Education, Sciences and Technology, Sports and Culture (MEXT) for Scientific Research (No. 25287046) and by MEXT Strategic Program for Innovative Research (SPIRE) Field 5 and Joint Institute for Computational Fundamental Science (JICFuS). This investigation has also been supported by the European Union and the State of Hungary and co-financed by the European Social Fund in the framework of TAMOP-4.2.4.A/ 2-11/1-2012-0001 'National Excellence Program'. S.A would like to thank the Wigner Research Center for Physics for its kind hospitality during his stay for this research project. S. A and J. B. would like to thank the Max-Planck-Institut für Physik for its kind hospitality during their stay for this research project.

## A Resonance parameters on the lattice

In this subsection we work in the broken symmetry phase with vanishing 6 or higher point couplings ( $G = G_{k \geq 4} = 0$ ) and zero external field ( $H = 0$ ). The denominator of the lattice  $\sigma$  propagator has the form:

$$\mathcal{D}(K) \equiv \hat{K}^2 \left( \frac{6}{U} + J_\infty(K)|_{M=0} \right) + 2\Sigma^2. \quad (\text{A.1})$$

Setting  $K = (K_0, \underline{0})$ ,  $w = \hat{K}_0^2$  and performing the  $Q_0$  integration in eq.(3.2) we obtain:

$$\mathcal{D}(w) \equiv \mathcal{D}(K)|_{K=(K_0, \underline{0})} = w \left( \frac{6}{U} + R(w) \right) + 2\Sigma^2, \quad (\text{A.2})$$

where

$$R(w) = \int_{-\pi}^{\pi} \frac{d^2 Q}{(2\pi)^2} \frac{v(Q)}{\hat{Q}^2(\hat{Q}^2 + 4) + w}, \quad v(Q) = \frac{\hat{Q}^2 + 2}{\sqrt{\hat{Q}^2(\hat{Q}^2 + 4)}} \quad (\text{A.3})$$

$R(w)$  is analytic in  $w$  with a cut starting at  $w = 0$  extending along the negative real axis to  $w = -96$ . It has the spectral representation:

$$R(w) = \int_0^{96} ds \frac{\rho(s)}{s + w}, \quad (\text{A.4})$$

with spectral function

$$\rho(s) = \frac{1}{4\pi^2 \sqrt{s}} K \left( \sqrt{1 - p(s)^2} \right), \quad (\text{A.5})$$

where

$$p(s) = \frac{1}{4} [6 - \sqrt{4 + s}], \quad (\text{A.6})$$

and  $K(k)$  is the elliptic function:

$$K(k) \equiv \int_0^{\pi/2} dt \frac{1}{\sqrt{1 - k^2 \sin^2(t)}}. \quad (\text{A.7})$$

We are interested in identifying a sigma resonance for bare parameters close to the continuum limit i.e. we seek zeros of  $\mathcal{D}(w)$  at small  $w = w^{(0)}$  on the second sheet:

$$w^{(0)} = -M_\sigma^2(1 - ir)^2, \quad (\text{A.8})$$

where  $r$  is the ratio of width to mass. Noting that on the first sheet the discontinuity across the cut is

$$R(-s - i\epsilon) - R(-s + i\epsilon) = 2\pi i \rho(s). \quad (\text{A.9})$$

we can analytically continue to the second sheet (at least to a region near the cut) according to

$$R^{(II)}(w) = R(w) + 2\pi i \rho(-w). \quad (\text{A.10})$$

The equations determining the resonance parameters are then given by

$$\frac{2\Sigma^2}{M_\sigma^2} = \frac{(1 + r^2)^2}{2r} \left[ -\mathcal{D}(M_\sigma^2, r) + 2\pi \Re \rho(-w^{(0)}) \right], \quad (\text{A.11})$$

$$\frac{6}{U} = -\mathcal{C}(M_\sigma^2, r) + 2\pi \Im \rho(-w^{(0)}) + \frac{(1 - r^2)}{2r} \left[ -\mathcal{D}(M_\sigma^2, r) + 2\pi \Re \rho(-w^{(0)}) \right], \quad (\text{A.12})$$

where

$$\mathcal{C}(M_\sigma^2, r) = \int_{-\pi}^{\pi} \frac{d^2Q}{(2\pi)^2} \frac{v(Q) \left\{ \hat{Q}^2 (\hat{Q}^2 + 4) - M_\sigma^2 (1 - r^2) \right\}}{\left\{ \hat{Q}^2 (\hat{Q}^2 + 4) - M_\sigma^2 (1 - r^2) \right\}^2 + 4r^2 M_\sigma^4}, \quad (\text{A.13})$$

$$\mathcal{D}(M_\sigma^2, r) = 2r M_\sigma^2 \int_{-\pi}^{\pi} \frac{d^2Q}{(2\pi)^2} \frac{v(Q)}{\left\{ \hat{Q}^2 (\hat{Q}^2 + 4) - M_\sigma^2 (1 - r^2) \right\}^2 + 4r^2 M_\sigma^4}. \quad (\text{A.14})$$

## B Finite-volume mass gap and running coupling

An interesting alternative running coupling is the LWW finite volume coupling[30] defined through the variable

$$z = \ell m(\ell), \quad (\text{B.1})$$

where  $\ell = La$  is the extension of the periodic box in physical units and  $m(\ell)$  is the particle mass when confined to the box,  $m_R = m(\infty)$ . Our purpose here is to show the robustness of the walking behavior of our model by demonstrating that the qualitative properties are the same whether we consider the infinite volume four-point coupling and corresponding beta function (as we did in the main text) or similar objects associated to the finite volume mass gap. In addition, in MC measurements the lattice size is always finite and we can make a virtue of necessity and use a finite volume coupling to study walking behavior.

Later we will also use the dimensionless volume variables

$$L_u = \ell u_{\text{eff}}, \quad L_m = \ell m_R, \quad \text{and} \quad L_w = \ell w_R. \quad (\text{B.2})$$

On the lattice, we consider the  $T \rightarrow \infty$  limit keeping  $L$  finite and  $H \rightarrow 0$ . We define

$$I(z, M(L)) = \frac{1}{L^2} \int_{-\pi}^{\pi} \frac{dK_0}{2\pi} \sum_{l_1, l_2} \frac{1}{\hat{\mathbf{K}}^2 + M^2(L)}. \quad (\text{B.3})$$

Fixing

$$z = LM(L) \quad (\text{B.4})$$

this has small  $M(L)$  expansion

$$I(z, M(L)) = I_0 + M(L)x_1(z) + O(M^2(L)), \quad (\text{B.5})$$

or written alternatively

$$\frac{I(z, M(L))}{a} = \frac{I_0}{a} + m(\ell) x_1(z) + O(a), \quad (\text{B.6})$$

where we have used that  $M(L) = m(\ell)a$ . The meaning of the terms in (B.6) is

$$\text{linear divergence} + \text{physical part} + \text{cutoff effects}. \quad (\text{B.7})$$

The linear divergence ( $I_0/a$ ) is the same as for infinite volume. The physical part of the result should be the same as for dimensional regularization where there is no linear divergence and gives the finite result:

$$x_1(z) = -\frac{1}{4\pi} + \frac{1}{4\pi z} J(z^2/4\pi). \quad (\text{B.8})$$

The definition of this function is

$$J(v) \equiv \int_0^\infty \frac{dt}{\sqrt{t^3}} e^{-vt} [S^2(1/t) - 1], \quad (\text{B.9})$$

where

$$S(x) = \sum_{n=-\infty}^{\infty} e^{-\pi n^2 x}. \quad (\text{B.10})$$

$J$  is positive and monotonically decreasing to 0. For small  $z$

$$J(z^2/4\pi) \approx \frac{2\pi}{z} + \text{const.} \quad (\text{B.11})$$

The function  $x_1(z)$  decreases from  $\infty$  to  $-1/4\pi$  and has small  $z$  behaviour

$$x_1(z) \approx \frac{1}{2z^2} + O(1/z). \quad (\text{B.12})$$

There is a unique zero of this function at some  $z = z_*$ .  $x_1(z)$  is positive for  $0 < z < z_*$  and negative for  $z > z_*$ . For later purposes we also note that the function  $zx_1(z)$  decreases from  $\infty$  to  $-\infty$  and  $x_1(z)/z$  also decreases (from  $\infty$  to 0) for  $0 < z < z_*$ .

### B.1 Continuum limit(s)

From the first gap equation (2.13) we get the expansion

$$\Omega_0 = I_0 + \omega_1 a + \omega_2 a^2 + \dots \quad (\text{B.13})$$

with

$$\omega_1 = \frac{zx_1(z)}{\ell}. \quad (\text{B.14})$$

Let us denote the analogous expansion coefficients for the infinite volume theory by  $\tilde{\omega}_i$ . The leading coefficient is:

$$\text{SYM} : \tilde{\omega}_1 = -\frac{m_R}{4\pi}, \quad \text{BRO} : \tilde{\omega}_1 = w_R. \quad (\text{B.15})$$

In addition, eq. (3.7) leads to

$$U''(I_0) = \left( \frac{u_{\text{eff}}}{12} - U'''(I_0)\tilde{\omega}_1 \right) a. \quad (\text{B.16})$$

From the second gap equation (2.14) we see that

$$\frac{R}{2} = 3 + \frac{M^2}{2} - \left( U'(\Omega_0) - \frac{R}{2} \right) \quad (\text{B.17})$$

has to be volume-independent. Although we do not need the actual value of couplings in the potential  $U(S)$ , their volume independence gives enough information to calculate the mass gap in finite volume.

The volume independence leads to the equation,

$$\frac{U'''(I_0)}{2}(2\tilde{\omega}_1\omega_1 - \omega_1^2) - \frac{u_{\text{eff}}}{12}\omega_1 + \frac{z^2}{2\ell^2} = \frac{U'''(I_0)}{2}\tilde{\omega}_1^2 - \frac{u_{\text{eff}}}{12}\tilde{\omega}_1 + \frac{m_R^2}{2}, \quad (\text{B.18})$$

where the right-hand side is volume-independent, so is the left-hand side. It is interesting to see that  $U'''(I_0)$  dependence appears in the equation for finite volume quantities, while such a  $U'''(I_0)$  dependence shows up only in the 6-pt vertex in the infinite volume, which is  $1/N$  suppressed compared to the 4-pt vertex, as already discussed before. For simplicity of the analysis, we set  $U'''(I_0) = 0$  in the remaining of this appendix.

As before, the case I is obtained from the case II in the  $u_{\text{eff}} \rightarrow \infty$  limit. We concentrate on the generic case II and we write (with  $U'''(I_0) = 0$ )

$$\frac{zx_1(z)}{6\ell} = \frac{w_R}{6} - \frac{m_R}{24\pi} + \frac{1}{u_{\text{eff}}} \left( \frac{z^2}{\ell^2} - m_R^2 \right). \quad (\text{B.19})$$

This formula is valid for both phases if we note that  $w_R = 0$  in the symmetric phase and  $m_R = 0$  in the broken phase. We now list the equation determining the finite volume mass gap in all cases.

- case IA

$$L_m = -4\pi zx_1(z)$$

- case IB

$$x_1(z) = 0$$

- IIA

$$z^2/L_u^2 - zx_1(z)/(6L_u) = \alpha^2 + \alpha/24\pi \quad \text{or} \quad \alpha z^2/L_m^2 - zx_1(z)/(6L_m) = \alpha + 1/24\pi$$

- IIB

$$L_u = 6z/x_1(z)$$

- IIC

$$zx_1(z) = L_w + \frac{\beta z^2}{8L_w}$$

- IC

$$zx_1(z) = L_w$$

From these formulas we find the following qualitative behaviours.

- case IA

$z$  goes from  $z_*$  to  $\infty$  as  $L_m$  goes from 0 to  $\infty$ . For small  $L_m$ ,  $z \simeq z_*$  so the model is UV conformal, as found before. For large  $L_m$ ,  $z \approx L_m$ .



- case IB

$z = z_*$  constant, the model is conformal.

- case IIA

$z$  moves from 0 to  $\infty$  as  $L_u$  (or  $L_m$ ) changes from 0 to  $\infty$ , the model is UV AF. For small  $L_u$ ,  $z \approx (L_u/12)^{1/3}$  and for large  $L_u$ ,  $z \approx L_m = \alpha L_u$ .

- case IIB

$z$  moves from 0 to  $z_*$  as  $L_u$  is changed from 0 to  $\infty$ , it is UV AF and IR conformal. For small  $L_u$  it also behaves as  $z \approx (L_u/12)^{1/3}$ .

- case IIC

For  $0 < L_w < z_1 \sqrt{\beta/8}$ ,  $z(L_w)$  is monotonically increasing from 0 to  $z_1$ , where  $z_1$  is defined by  $x_1(z_1) = \sqrt{\beta/2}$ . For small  $L_w$ ,  $z \approx (4L_w/\beta)^{1/3}$ . This model is also UV AF. For  $L_w > z_1 \sqrt{\beta/8}$ ,  $z(L_w)$  is monotonically decreasing and for large  $L_w$ ,  $z \approx 1/(2L_w)$ .

- case IC

$z(L_w)$  is monotonically decreasing,  $z(0) = z_*$ , the model is UV conformal. For large  $L_w$ ,  $z \approx 1/(2L_w)$ .

## B.2 Finite volume coupling

Now we can define the finite volume running coupling  $g_{FV}$  by

$$g_{FV} = \frac{48(z/z_*)^3}{p + (1-p)(z/z_*)^2}, \quad (\text{B.20})$$

where  $p$  is some constant. It is normalized to 48 for the conformal points and has qualitatively the same behaviour as  $g_4$  and also the corresponding beta function

$$\beta_{FV}(g_{FV}) = -L_u \frac{\partial}{\partial L_u} g_{FV}(L_u) \quad (\text{B.21})$$

shows walking behaviour for small  $\alpha$ . Fig. 5 gives  $\beta_{FV}(g_{FV})$  as a function of  $g_{FV}$  at three values of  $b$ . Like the beta function of the 4-pt coupling in the text, the "walking" behavior in the finite volume coupling becomes more visible, as  $b$  decreases.

## References

- [1] S. Weinberg, Phys. Rev. D19 (1979) 1277
- [2] L. Susskind, Phys. Rev. D20 (1979) 2619
- [3] C. Hill, E. Simmons, Phys. Rep.381 (2003) 235
- [4] S. Dimopoulos, L. Susskind, Nucl. Phys. B155 (1979) 237
- [5] E. Eichten, K. Lane, Phys. Lett. B90 (1980) 125

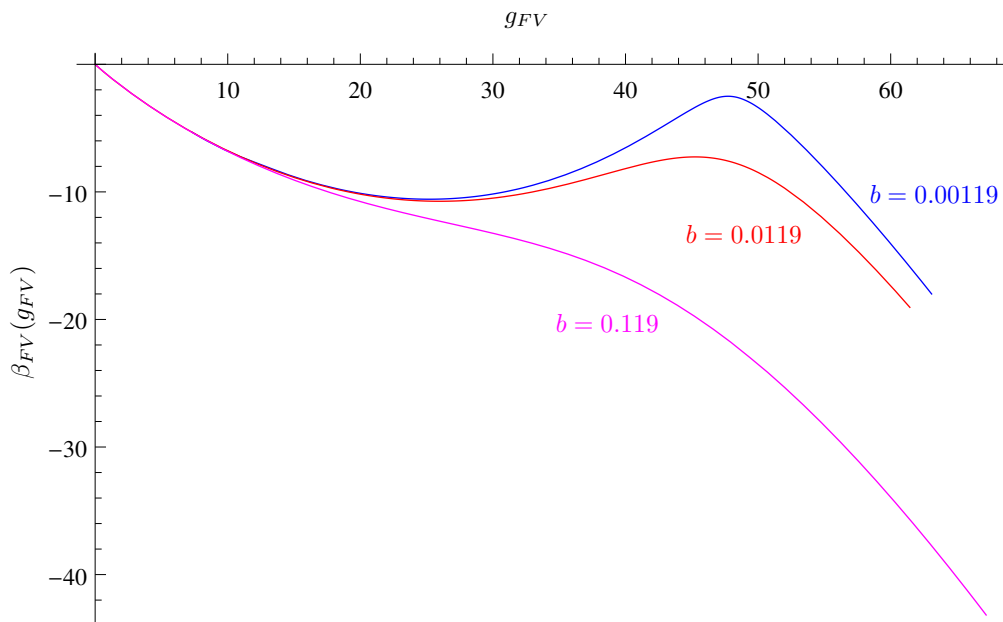


**Figure 5.** The beta function  $\beta_{FV}(g_{FV})$  as a function of the finite volume coupling  $g_{FV}$  at  $b \equiv 96\alpha = 0.119$  (magenta line), 0.0119 (red line) and 0.00119 (blue line).

- [6] M. E. Peskin and T. Takeuchi, Phys. Rev. D46 (1992) 381
- [7] B. Holdom, Phys. Lett. B150 (1985) 301
- [8] K. Yamawaki, M. Bando, K-i. Matumoto, Phys. Rev. Lett. 56 (1986) 1335
- [9] T. Appelquist, L. C. R. Wijewardhana, Phys. Rev. D35 (1987) 774
- [10] T. Banks, A. Zaks, Nucl. Phys. B196 (1982) 189
- [11] T. Appelquist, G. T. Fleming, E. T. Neil, Phys. Rev. Lett. 100 (2008) 171607, Erratum-ibid. 102 (2009) 149902
- [12] G. T. Fleming, PoS (Lattice 2008) 021
- [13] E. Pallante, PoS (Lattice 2009) 015
- [14] L. Del Debbio, PoS (Lattice 2010) 004
- [15] E. Neil, PoS (Lattice 2011) 009
- [16] D. Negradi, PoS (Lattice 2011) 010
- [17] J. Giedt, PoS (Lattice 2012) 006
- [18] J. Kuti, PoS (Lattice 2013) 004
- [19] E. Itou, PoS (Lattice 2013) 005

- [20] LatKMI Collaboration (Yasumichi Aoki et al.), Phys.Rev. D87 (2013) 9, 094511; K. Nagai, PoS LATTICE2013 (2014) 071.
- [21] A. Hasenfratz, A. Cheng, G. Petropoulos, D. Schaich Conference: C12-12-04, p.44-50 Proceedings, arXiv:1303.7129
- [22] J. Giedt, E. Weinberg, Phys. Rev. D85 (2012) 097503
- [23] S. Catterall, L. Del Debbio, J. Giedt , L. Keegan, Phys.Rev. D85 (2012) 094501
- [24] D. Nogradi, JHEP 1205 (2012) 089
- [25] P. de Forcrand, M. Pepe, U. J. Wiese, Phys.Rev. D86 (2012) 075006 and PoS LATTICE2012 (2012) 041
- [26] M. Moshe, J. Zinn-Justin, Phys.Rept. 385 (2003) 69-228
- [27] F. David, D. A. Kessler, H. Neuberger, Phys. Rev. Lett. 53 (1984) 2071
- [28] F. David, D. A. Kessler, H. Neuberger, Nucl. Phys. B257 (1985) 695
- [29] D. A. Kessler, H. Neuberger, Phys. Lett. B157 (1985) 416
- [30] M. Lüscher, P. Weisz, U. Wolff, Nucl.Phys. B359 (1991) 221